Dalton Transactions

Ruthenium(II)-polypyridyl doped zirconium(IV) metal-organic frameworks for solid-state electrochemiluminescence

Journal:	*Dalton Transactions*
Manuscript ID	DT-ART-09-2018-003906.R1
Article Type:	Paper
Date Submitted by the Author:	30-Oct-2018
Complete List of Authors:	Cai, Meng; Virginia Tech, Chemistry Loague, Quentin; Virginia Tech, Chemistry Zhu, Jie; Virginia Polytechnic Institute and State University, Chemistry; University of California San Diego, Chemistry and biochemistry Lin, Shaoyang; Virginia Tech, Chemistry; Virginia Tech, Usov, Pavel; Virginia Tech, Chemistry Morris, Amanda; Virginia Tech, Chemistry

Journal Name

ARTICLE

Ruthenium(II)-polypyridyl doped zirconium(IV) metal-organic frameworks for solid-state electrochemiluminescence

Meng Cai, Quentin Loague, Jie Zhu, Shaoyang Lin, Pavel M. Usov and Amanda J. Morris*

Received 00th January 20xx,
Accepted 00th January 20xx

DOI: 10.1039/x0xx00000x

www.rsc.org/

Solid-state electrochemiluminescence (ECL) has drawn increasing attention due to their advantages over solution-phase ECL, such as reducing consumption of expensive reagent and enhancing the ECL signal. Herein we report the ruthenium(II)-polypyridyl doped zirconium(IV) metal-organic framework (MOF) film, UiO-67-Ru@FTO, for solid-state electrochemiluminescence. With tripropylamine (TPA) as coreactant, UiO-67-Ru@FTO exhibited high ECL intensity and good stability. A linear relationship was found between ECL intensity and TPA concentration in a wide range of 0.04-20 mM. Additionally, UiO-67-Ru@FTO was successfully used for dopamine detection, implying its great potential for real-life application.

Introduction

Electrochemiluminescence (ECL), also known as electrogenerated chemiluminescence, is a class of luminescence produced when electrochemically generated intermediates undergo electron-transfer reactions to form excited states that emit light.[1-3] Unlike conventional chemiluminescence that is typically initiated and controlled by careful fluid flow of mixing reactive species, ECL is triggered and manipulated by the potential applied on electrodes. This allows for accurate control over the time and position of the light-emitted reactions. The combination of the advantages of both electrochemistry and chemiluminescence has rendered ECL an exceptional detection technique with excellent sensitivity, selectivity and reproducibility. ECL has been widely used in DNA analyses, clinical diagnostics, water testing, etc.[4-10] Among various ECL luminophores, metal complexes, especially tris(2,2'-bipyridine) ruthenium(II) [$Ru(bpy)_3^{2+}$] and its derivatives, occupy the majority of research. They exhibit good stability in both organic solvents and water, they have long-lived exited states, and they undergo reversible one-electron transfer reactions at easily attainable potentials.[11] In early studies, Ru complexes were used in homogeneous solution, an approach which limits re-use. Different approaches of heterogenizing ECL luminophores onto substrates have been extensively investigated, such as polymer-composite films, nanostructure-based films, Langmuir–Blodgget films, and sol-gel composites.[12-15]

Metal-organic frameworks (MOFs) are a class of crystalline porous materials composed of metal ions or clusters as secondary building units (SBUs) coordinated to multi-dentate organic ligands. Their unique features, including high surface areas, well-defined uniform nano-scale pores and channels and good thermal/chemical stability, have made MOFs a promising platform material for ECL due to following reasons. 1) ECL luminophores can be easily immobilized into well-organized nanostructured framework by serving as building units or/and guest molecules of MOFs. This strategy eliminates need for additional binding agent, such as cation-exchange polymer Nafion that has been widely used to attach ECL luminophores to electrodes.[16-19] 2) The immobilization of ECL luminophores using binding agents may rely on electrostatic interactions. For instance, Dang *et al.* fabricated chitosan/$Ru(bpy)_3^{2+}$/silica nanoparticles modified electrode by making use of the electrostatic interaction between Nafion (with negative charges on the surface) and chitosan (with positive charges on the surface).[14] In comparison, the coordination between luminophore and MOF structure is strong, which can greatly decrease the chance of chromophore leaching and thereby increase the durability. 3) The interconnected pores and channels in MOFs enable a high concentration of active luminophores to be immobilized within a small geometric area. Thus, ECL intensity can be enhanced compared to traditional heterogenizing approaches. Studies have shown that redox charge hopping through MOFs, enables electrons to transport throughout the entire MOF structure during electrochemical reactions.[20-22] Thus, the incorporation of ECL luminophores into MOFs is promising to inspire new ECL detector fabrication strategy.

To date, only a few reports have been published on the immobilization of Ru complexes in MOFs for ECL. Park *et al.* prepared a redox-active zinc-adeninate MOF via post-synthetic cation exchange with $Ru(bpy)_3^{2+}$, but a rapid decay in ECL intensity due to structural decomposition was observed.[23] Xu *et*

[a] Department of Chemistry, Virginia Polytechnic Institute and State University, 800 W. Campus Drive Blacksburg, Virginia 24061, United States
E-mail: ajmorris@vt.edu.
[b]

† Footnotes relating to the title and/or authors should appear here.
Electronic Supplementary Information (ESI) available: [details of any supplementary information available should be included here]. See DOI: 10.1039/x0xx00000x

al. synthesized an ECL detector prepared from {Ru[4,4'-$(HO_2C)_2$-bpy]$_2$bpy}$^{2+}$ and Zn^{2+}.[19] However, the detector was prepared by drop-casting the mixture of MOF and graphene oxide (GO) onto a glassy carbon electrode, of which the reusability after long-time cycling can be an issue.

Herein, we report a self-assembled redox-active MOF film, UiO-67-Ru@FTO for solid-state ECL. The thin film (UiO-67-Ru@FTO) has been prepared following a reported procedure.[24] The MOF film was grown on fluorine-doped tin oxide (FTO) glass slide solvothermally by doping $Ru(bpy)_2(dcbpy)Cl_2$ (bpy=2,2'-bypyridine, dcbpy=5,5'-dicarboxy-2,2'-bipyridine), RuDCBPY, into Zr-based MOF UiO-67, $Zr_6O_4(OH)_4(bpdc)_6$ (bpdc=biphenyldicarboxylic acid). With tripropylamine (TPA) as coreactant, UiO-67-Ru@FTO exhibited high ECL intensity and good stability. In addition, UiO-67-Ru@FTO was also used for dopamine (DA) detection.

Results and Discussion

Synthesis and characterization

Incubation of a FTO slide yields the growth of a crystalline thin film of UiO-67-Ru on the FTO surface. Scanning electron microscopy (SEM) images reveal that the entire film is composed of uniformly distributed MOF particles of octahedral structure with an average size of ~500 nm (Fig. 1A and 1B), which is reminiscent of classical structure of UiO series MOFs. Cross-section SEM shows that the thickness of MOF film is ~20 µm (Fig. 1C). Powder X-ray Diffraction (PXRD) patterns of UiO-67-Ru powders show a close match to simulated PXRD patterns of UiO-67, indicating that as-prepared UiO-67-Ru has inherited the crystal structure of UiO-67 (Fig. 1D). No additional peaks were observed, indicating absence of crystalline impurities. The MOF powder has a Brunauer-Emmett-Teller (BET) specific surface area of 927 $m^2\ g^{-1}$, lower than that of parent UiO-67 due to the incorporation of Ru^{2+} linkers (Fig. S1). The high surface area indicates the highly porous structure of as-prepared UiO-67-Ru film, which is expected to facilitate efficient diffusion of reactants.

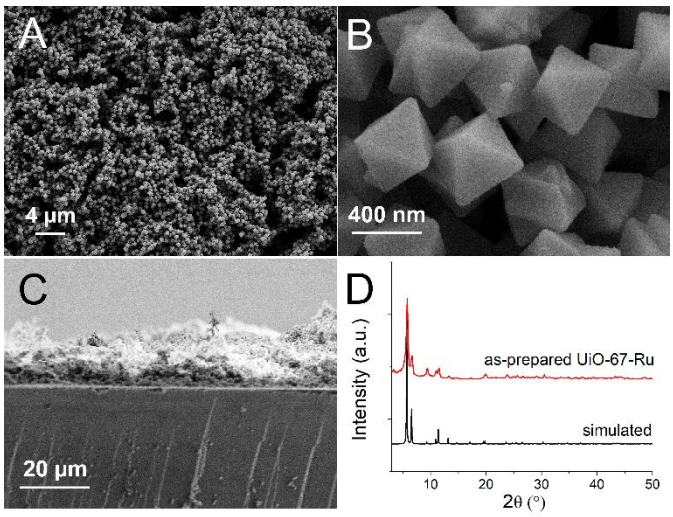

Fig. 1 (A, B) SEM images of the surface and (C) the cross-section of UiO-67-Ru film. (D) PXRD patterns of UiO-67-Ru powders.

Photophysical characterization

Photophysical properties of UiO-67-Ru thin film were first investigated by ultraviolet-visible spectroscopy (UV-Vis) (Fig. S2). An absorbance peak at ~450 nm was observed in the diffuse reflectance spectrum, corresponding to the singlet metal-to-ligand charge transfer state, ^{1}MLCT. This is in good agreement with the d_π^6 to $d_\pi^5\pi^*$ transition reported for $Ru(bpy)_3^{2+}$ and its derivatives,[25-27] implying the successful introduction of $Ru(bpy)_2(dcbpy)Cl_2$ into MOFs. With light excitation at 450 nm, UiO-67-Ru@FTO in acetonitrile (MeCN) displays a steady-state emission maximum at ~650 nm, which corresponds to relaxation of the ^{3}MLCT state (Fig. S3). Compared to the emission spectrum of ligand $Ru(bpy)_2(dcbpy)Cl_2$ in MeCN, the maximum of MOF film red-shifted. This is partially caused by the difference between a solid-state and a solution-based chemical environment. Furthermore, this can also be attributed to the existence of two populations of RuDCBPY in UiO-67 framework that has been investigated in a previous study from our group.[24] It was reported that at lower doping concentrations (<10 m*m*), RuDCBPY would incorporate into the larger octahedral cavity of the framework as the organic linker. Upon increasing doping, RuDCBPY can also be encapsulated in the octahedral cavities in addition to incorporation. This was supported by not only red shift in emission spectra from higher doping UiO-67-Ru, but also the switch from single exponential to biexponential decay from emission lifetime data with increasing doping. ICP-MS results of digested MOF films (see Experimental section for detail) indicate the doping concentration of Ru is ~ 18 m*m*, which falls in higher doping range based on previous study. Therefore, it is postulated that there exist both incorporated and encapsulated RuDCBPY in as-prepared UiO-67-Ru@FTO films.

Electrochemical characterization

The electrochemical behavior of UiO-67-Ru@FTO was investigated prior to electrochemiluminescence studies. Cyclic voltammetry (CV) was conducted in MeCN containing 0.1 M $LiClO_4$ as electrolyte. For comparison, an undoped UiO-67 thin film on FTO (UiO-67@FTO) and a bare FTO were also investigated. In the absence of TPA, no obvious peak was observed from a bare FTO in the potential window of -0.12 to 1.68 V versus ferrocene/ferrocene$^+$ (Fc/Fc^+) (Fig. 2), indicating good stability of FTO and electrolyte under such electrochemical measurements. A redox wave is observed with a half-wave potential of 1.00 V in the CV of UiO-67-Ru@FTO, corresponding to the Ru^{2+}/Ru^{3+} couple of the incorporated RuDCBPY, which further verifies the presence of the chromophore in the as-prepared MOF thin film. In the presence of 20 mM TPA, the CVs of bare FTO, UiO-67@FTO and UiO-67-Ru@FTO all display an increase on anodic current starting from 0.35 V, which is ascribed to the oxidation of TPA.[28] The undoped UiO-67 thin film showed a lower current than bare FTO. This is presumably because the coverage of undoped MOF decreased the number of accessible conductive sites on FTO. It can be seen that UiO-67-Ru@FTO exhibited a very similar current for TPA oxidation as to that of bare FTO. This implies that the incorporation of Ru complexes in UiO-67 MOF enables efficient electron transfer. No obvious oxidation peak of Ru^{2+} was seen from UiO-67-Ru@FTO, which is due to that the oxidation current has merged into that of TPA oxidation. In addition, no reduction peak was seen, indicating the presence of an alternative route for Ru^{3+}/Ru^{2+} transformation. In a typical

solution-based $Ru(bpy)_3^{2+}$/TPA system, ECL can be generated via the so-called "oxidative reduction" route, in which both TPA and $Ru(bpy)_3^{2+}$ are oxidized, and the resulting radical $TPA^{\bullet}$ and $Ru(bpy)_3^{3+}$ can react to give $Ru(bpy)_3^{2+*}$ that is ready to emit light. Similarly, in our UiO-67-Ru/TPA system, when applied potential is increasing beyond 0.77 V, both TPA and Ru^{2+} are oxidized, and the resulting Ru^{3+} will be reduced by $TPA^{\bullet}$. As a result, on the return scan there is no Ru^{3+} to reduce and a cathodic peak is not observed.

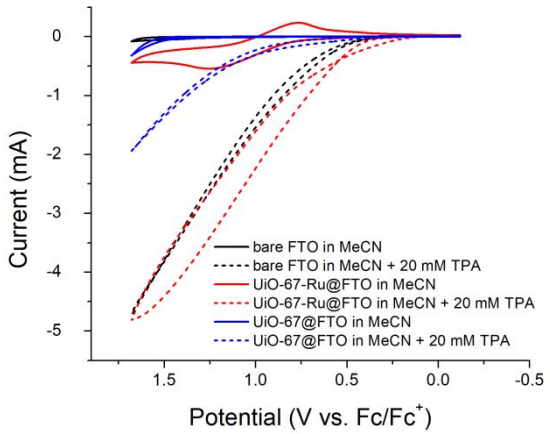

Fig. 2 CVs of bare FTO (black), UiO-67-Ru@FTO (red), and UiO-67@FTO (blue) in the absence (solid line) or presence (dotted line) of 20 mM TPA in MeCN containing 0.1 M $LiClO_4$ at the scan rate of 100 mV s^{-1}.

To yield high ECL intensity, it is necessary to provide considerable amount of Ru^{3+} upon applying a voltage. As a result, efficient charge transport throughout the whole framework is crucial. As UiO-67 MOFs are made from redox-inactive Zr(IV) clusters and dicarboxylic acid linkers, they are expected to be intrinsically insulating. With Ru doped in UiO-67-Ru@FTO film, however, efficient charge transport is made possible *via* redox hopping. Initially proposed as a charge transport mechanism for linear conductive polymers,[29-31] redox hopping was also found to dominate charge transfer in several redox-active MOFs. For instance, in a previous study by Morris et al.,[32] charge could hop from one electroactive site to another, leading to a diffusion-controlled current behavior, which obeys the Randles-Sevcik equation:

$$i_p = 0.4463nFAC\left(\frac{nFvD}{RT}\right)^{1/2} \quad (1)$$

where i_p is the anodic/cathodic peak current, n is the number of electrons transferred in the redox reaction, $F$is the Faraday constant, A is the electrode area, C is the concentration of the electroactive species, v is the scan rate, D is the diffusion coefficient, R is gas constant, and T is temperature.

This equation indicates a linear relationship between i_p and $v^{1/2}$, or, a linear dependence of $\log(i_p)$ on $\log(v)$ with a slope of 0.5. To elucidate the mechanism of charge transport in UiO-67-Ru@FTO films, CVs of UiO-67-Ru@FTO at various scan rates ranging from 10 to 1000 mV s^{-1} were collected (Figure 3A), and the logarithms of the cathodic and anodic peak currents were plotted against the logarithm of scan rates (Figure 3B). As seen, a linear relationship between the logarithm of the peak current and the logarithm of the scan rate was obtained with a slope of ~0.5.This result implies that charge can hop between redox-active Ru sites and "diffuse" deep inside the MOF film.

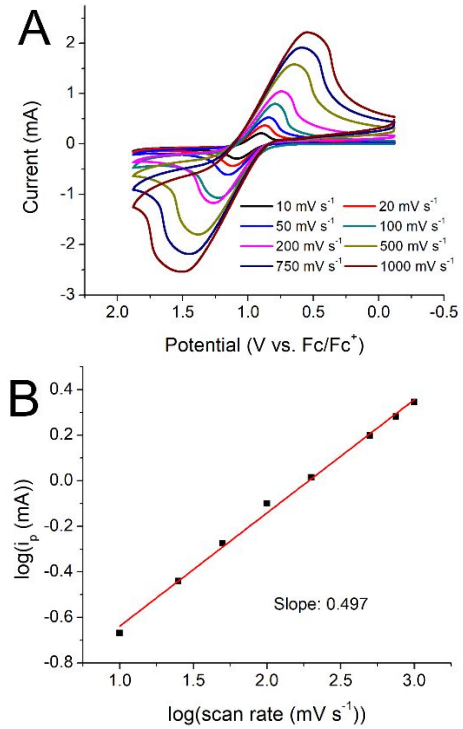

Fig. 3 (A) CVs of UiO-67-Ru@FTO in MeCN containing 0.1 M $LiClO_4$ at the scan rate ranging from 10 to 1000 mV s^{-1}; (B) The plot of the logarithm of peak currents (absolute values) versus the logarithm of scan rates.

Electrochemiluminescence study

The ECL behavior of UiO-67-Ru@FTO was first investigated at a controlled potential of 1.68 V. This applied potential is sufficient to oxidize both RuDCBPY and TPA (Fig. 4A). An emission maximum at ~660 nm was observed, consistent to the observed photoluminescence of RuDCBPY. The ECL-potential curves (ECL responses plotted versus applied potentials) collected with various TPA concentrations (0.04 mM-20 mM) are shown in Fig. 4B. ECL intensities in the presence of TPA increase as a function of higher applied anodic potential above 0.77 V, at the onset of Ru^{2+} oxidation. The ECL response increases with increasing TPA concentration, and the relationship of ECL peak intensity versus TPA concentration is illustrated in Fig. 4C. A good linear relationship (see ESI for more detail) was obtained with TPA concentration ranging from 0.04 mM to 20 mM in which each point represents five repeated measurements.

To gain more insights into the ECL performance of our UiO-67-Ru thin film, the amount of active Ru^{2+} sites involved in ECL was estimated by amperometry (Fig. S4). It was assumed that the charge that passed during the controlled-potential electrolysis was due to one-electron transfer process of Ru^{2+}/Ru^{3+} redox couple. The current obtained from undoped UiO-67 thin film was subtracted as background correction. It was also assumed that all electroactive Ru^{2+} sites contributed to the ECL. As a result, the coverage of ECL-active Ru^{2+} was calculated to be (0.93±0.04) × 10^{-7} mol·cm^{-2} (see ESI for calculation detail). The overall loading of the film was (1.39±0.07) × 10^{-7} mol·cm^{-2}, determined by ICP-MS. Based on above results, (67.2±0.4)% Ru^{2+} in the film was electroactive. For comparison, same amount of RuDCBPY ligand as the total loading of Ru^{2+} in the film was dissolved in solution, and ECL of

solution-based $Ru(bpy)_3^{2+}$/TPA system was obtained following a similar pattern with a bare FTO as a working electrode (Fig. S5). With the presence of 20 mM TPA, lower intensity was observed from solution-based system compared to that of ECL generated from UiO-67-Ru@FTO, indicating higher availability of Ru^{2+} in our MOF ECL system.

Good reproducibility and stability are critical factors for evaluating ECL detector performance. The ECL response of UiO-67-Ru@FTO in the presence of 20 mM TPA upon consecutive cyclic scans demonstrated constant signal intensities with relative standard deviation (RSD) of 2.3%, indicating good repeatability of as-prepared UiO-67-Ru film (Fig. 4D). SEM after ECL shows no observable structural change, indicating good durability of MOF film (Fig. S6). In addition, little leaching of Ru (< 2%) was detected in resulting solution after ECL by ICP-MS, which further verifies the good stability of as-prepared MOF film.

Based on the electrochemical behavior and ECL profile of UiO-67-Ru@FTO discussed above, we believe ECL in our UiO-67-Ru/TPA system happens via the mechanism proposed below. When applied potential is higher than 0.77 V, Ru^{2+} incorporated in UiO-67, [UiO-67-Ru^{2+}] is oxidized to [UiO-67-Ru^{3+}] and TPA is oxidized to produce $TPA^{\bullet+}$. $TPA^{\bullet+}$ deprotonates spontaneously to generate $TPA^{\bullet}$. $TPA^{\bullet}$ then reduces [UiO-67-Ru^{3+}] to yield [UiO-67-Ru^{2+}*] that emits light:

$$[\text{UiO-67-Ru}^{2+}] \rightarrow [\text{UiO-67-Ru}^{3+}] + e^- \quad (2)$$

$$\text{TPA} \rightarrow \text{TPA}^{\bullet+} + e^- \quad (3)$$

$$\text{TPA}^{\bullet+} \rightarrow \text{TPA}^{\bullet} + H^+ \quad (4)$$

$$[\text{UiO-67-Ru}^{3+}] + \text{TPA}^{\bullet} \rightarrow [\text{UiO-67-Ru}^{2+}*] + P_1 \quad (5)$$

$$[\text{UiO-67-Ru}^{2+}*] \rightarrow [\text{UiO-67-Ru}^{2+}] + h\nu \quad (6)$$

(where $P_1 = (CH_3CH_2CH_2)N^+{=}CHCH_2CH_3$)

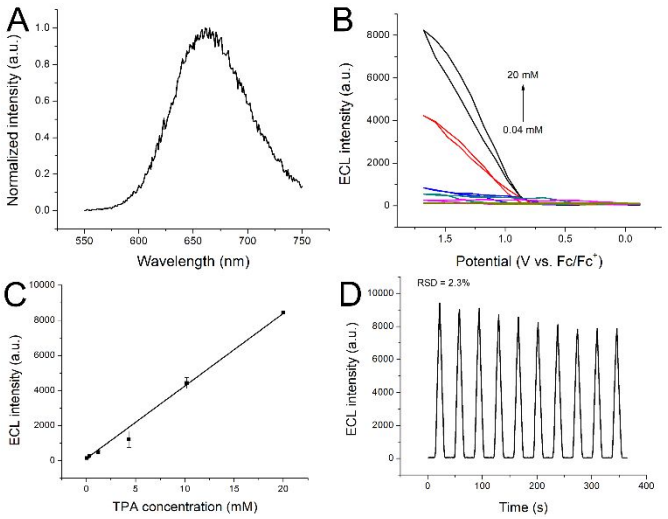

Fig. 4 (A) ECL profile of UiO-67-Ru@FTO in the presence of 20 mM TPA in MeCN containing 0.1 M $LiClO_4$ with a controlled potential at 1.68 V; (B) ECL-potential profiles of UiO-67-Ru@FTO with various TPA concentrations ranging from 0.04 to 20 mM; (C) calibration curve of ECL peak intensity versus TPA concentration; (D) time-based ECL of UiO-67-Ru@FTO in the presence of 20 mM TPA in MeCN containing 0.1 M $LiClO_4$ for 10 consecutive scans at a scan rate of 100 mV s^{-1}.

In order to evaluate the performance of UiO-67-Ru@FTO as a solid-state ECL detector, the detection of dopamine (DA), an important chemical messenger for our nervous system, via ECL quenching effect was investigated. It has been reported that $TPA^{\bullet}$ can be consumed by the oxidation product of DA before reacting with Ru^{3+}.[18] As a result, the ECL intensity should decrease as DA concentration increases. As expected, a decrease on ECL intensity from UiO-67-Ru@FTO was seen with addition of DA, and the relationship between ECL intensity and DA concentrations was plotted (Fig. 5, also see ESI). This result has suggested the potential of our UiO-67-Ru@FTO as a solid-state ECL detector for real-life applications, and further research will be carried out to investigate the selectivity and achieve wider detection range and lower limit of detection (LOD) by optimizing our UiO-67-Ru@FTO ECL system.

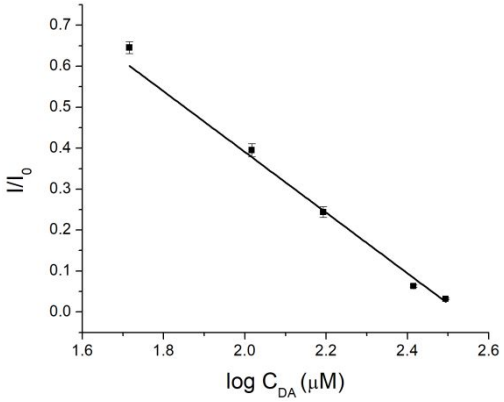

Fig. 5 The calibration curve of ECL intensity versus DA concentration in the presence of 20 mM TPA in MeCN containing 0.1 M $LiClO_4$

Conclusions

In summary, a self-assembled ruthenium(II)-polypyridyl doped zirconium(IV) metal-organic framework film, UiO-67-Ru@FTO, was successfully fabricated, and used for solid-state ECL. As-prepared UiO-67-Ru@FTO demonstrated high ECL with various TPA concentrations in a large range, and a linear relationship between ECL peak intensity and TPA concentration was obtained. Little ECL signal decay over 10 consecutive scans and negligible leaching of Ru^{2+} were observed, indicating good repeatability and stability of UiO-67-Ru@FTO. The MOF film has successfully combined the advantages of homogeneous ECL and heterogeneous MOF platforms. This work suggests that the incorporation of ECL luminophores into MOFs is a promising strategy to develop new ECL systems.

Experimental Section

Materials

All chemicals and solvents unless denoted were used as obtained without further purification, including cis-dichlorobis(2,2′-bipyridine)ruthenium(II) ($Ru(bpy)_2Cl_2$, Sigma-Aldrich, 97%), 2,2′-bipyridyl-5,5′-dicarboxylic acid (dcbpy, Ark Pharm, Inc., 95+%), 4,4′-biphenyldicarboxylic acid (BPDC, TCI, 97%), zirconium chloride, ($ZrCl_4$, Sigma-Aldrich, 98%), N,N-dimethylformamide (DMF, Fisher Scientific, HPLC grade > 99 %),

difluoroacetic acid (Fisher Chemical, 98%), sodium hydroxide (NaOH, Spectrum, 97%), acetone, (Spectrum, HPLC grade). Acetonitrile (MeCN, Fisher Scientific, HPLC grade) was distilled to yield anhydrous MeCN for use in all electrochemical measurements.

Synthesis of $[Ru(bpy)_2(dcbpy)]Cl_2$ (RuDCBPY)

RuDCBPY was synthesized according to a previous report.[33] $Ru(bpy)_2Cl_2$ (160 mg, 0.33 mmol) was mixed with dcbpy (101 mg, 0.42 mmol) in 20 mL of EtOH/water (1:1 v/v), refluxed for 12 h. The resulting product was concentrated and recrystallized from mixture of methanol/diethyl ether. ^{1}H NMR (DMSO-d_6): δ 9.00 (d, 2H), 8.86 (m, 4H), 8.50 (d, 2H), 8.18 (m, 4H), 7.97 (s, 2H), 7.80 (d, 4H), and 7.53 (m, 4H).

Fabrication of UiO-67-Ru films and powders

0.1 mmol of $ZrCl_4$, 0.05 mmol of RuDCBPY, 0.05 mmol of BPDC ligand and 90 µL of difluoroacetic acid were dissolved in 10 mL DMF in a 6-dram vial. The mixture was sonicated for 10 min, and a clean fluorine-doped tin oxide (FTO) glass slide was placed inside. The vial was then heated at 120 °C for 24 h. After cooling to room temperature, the FTO with MOF growing on it (UiO-67-Ru@FTO) was washed with DMF and acetone to remove unreacted materials followed by soaking in acetone for 2 days. The solid product was collected by centrifugation and washed with DMF and acetone. The MOF powder was soaked in acetone for 2 days to remove the residual DMF in MOF pores. The final product was collected by centrifugation, washed with acetone, and then air-dried at room temperature.

SEM

Scanning electron microscopy (SEM) images were collected using a Leo/Zeiss 1550 field-emission scanning electron microscope.

PXRD

Powder X-ray Diffraction (PXRD) patterns were obtained with Rigaku Miniflex instrument (Cu Kα, λ = 1.5418 Å).

ICP-MS

To determine ruthenium and zirconium content in UiO-67-Ru film, the MOF film was digested in 70 % nitric acid and the solution was diluted 10 times with water. The resultant solution was tested using a Thermo Electron X-Series inductively coupled plasma mass spectrometer (ICP-MS).

N_2 adsorption

The N_2 adsorption were collected on a Quantachrome Autosorb-1, and the Brunauer-Emmett-Teller (BET) specific surface area was calculated from the relative pressure range of 0.05-0.3.

Electrochemical measurements

Electrochemical measurements were carried out with an EC epsilon potentiostat (BASi) using a three-electrode setup. A UiO-67-Ru@FTO, a platinum mesh and a non-aqueous Ag/Ag^+ reference electrode were used as the working, counter and reference electrodes, respectively. Anhydrous MeCN containing 0.1 M $LiClO_4$ was used as electrolyte. The solution was purged for 30 min before each measurement. All potentials were converted to be versus ferrocene/ferrocene$^+$ (Fc/Fc^+).

Photochemical and ECL studies

Absorption spectra were collected with a Cary series UV-Vis-NIR spectrophotometer from Agilent Technologies. The steady-state emission spectra and ECL profiles were collected using a PTI Felix 32 Spectrofluorimeter.

Conflicts of interest

There are no conflicts to declare.

Acknowledgements

This material is based upon work supported by the National Science Foundation under Grant No. 1551964. The authors would like to thank Dr. Jeffrey L. Parks for providing the ICP-MS data.

Notes and references

1 W. Miao, *Chem. Rev.*, 2008, **108**, 2506-2553.
2 M. M. Richter, *Chem. Rev.*, 2004, **104**, 3003-3036.
3 A. J. Bard, *Electrogenerated chemiluminescence*, CRC Press, New York, 2004.
4 L. W. Cheng and L. H. Stanker, *J. Agric. Food. Chem.*, 2013, **61**, 755-760.
5 R. Phillips and D. Abbott, *Food Addit. Contam.*, 2008, **25**, 1084-1088.
6 D. Tian, C. Duan, W. Wang, N. Li, H. Zhang, H. Cui and Y. Lu, *Talanta*, 2009, **78**, 399-404.
7 Y. Li, C. Wang, J. Sun, Y. Zhou, T. You, E. Wang and Y. Fung, *Anal. Chim. Acta*, 2005, **550**, 40-46.
8 S. Carrara, A. Aliprandi, C. F. Hogan and L. De Cola, *J. Am. Chem. Soc.*, 2017, **139**, 14605-14610.
9 R.-F. Huang, H.-X. Liu, Q.-Q. Gai, G.-J. Liu and Z. Wei, *Biosens. Bioelectron.*, 2015, **71**, 194-199.
10 A. Chen, G.-F. Gui, Y. Zhuo, Y.-Q. Chai, Y. Xiang and R. Yuan, *Anal. Chem.*, 2015, **87**, 6328-6334.
11 A. Juris, V. Balzani, F. Barigelletti, S. Campagna, P. Belser and A. von Zelewsky, *Coord. Chem. Rev.*, 1988, **84**, 85-277.
12 Z. Guo, Y. Shen, F. Zhao, M. Wang and S. Dong, *Analyst*, 2004, **129**, 657-663.
13 Y. Tao, Z. J. Lin, X. M. Chen, X. Chen and X. R. Wang, *Anal. Chim. Acta*, 2007, **594**, 169-174.
14 J. Dang, Z. Guo and X. Zheng, *Anal. Chem.*, 2014, **86**, 8943-8950.
15 G. Y. Zhang, C. Cai, S. Cosnier, H. B. Zeng, X. J. Zhang and D. Shan, *Nanoscale*, 2016, **8**, 11649-11657.
16 I. Rubinstein and A. J. Bard, *J. Am. Chem. Soc.*, 1980, **102**, 6641-6642.

17 I. Rubinstein and A. J. Bard, *J. Am. Chem. Soc.*, 1981, **103**, 512-516.
18 Q. Li, J. Y. Zheng, Y. Yan, Y. S. Zhao and J. Yao, *Adv. Mater.*, 2012, **24**, 4745-4749.
19 Y. Xu, X. B. Yin, X. W. He and Y. K. Zhang, *Biosens. Bioelectron.*, 2015, **68**, 197-203.
20 S. R. Ahrenholtz, C. C. Epley and A. J. Morris, *J. Am. Chem. Soc.*, 2014, **136**, 2464-2472.
21 H.-J. Son, S. Jin, S. Patwardhan, S. J. Wezenberg, N. C. Jeong, M. So, C. E. Wilmer, A. A. Sarjeant, G. C. Schatz and R. Q. Snurr, *J. Am. Chem. Soc.*, 2013, **135**, 862-869.
22 P. M. Usov, C. Fabian and D. M. D'Alessandro, *Chem. Commun.*, 2012, **48**, 3945-3947.
23 J. E. Park, H. Oh, J. An and I. S. Shin, *Bull. Korean Chem. Soc.*, 2017, **38**, 471-476.
24 W. A. Maza, S. R. Ahrenholtz, C. C. Epley, C. S. Day and A. J. Morris, *The Journal of Physical Chemistry C*, 2014, **118**, 14200-14210.
25 A. Juris, S. Campagna, V. Balzani, G. Gremaud and A. Von Zelewsky, *Inorg. Chem.*, 1988, **27**, 3652-3655.
26 P.-H. Xie, Y.-J. Hou, B.-W. Zhang, Y. Cao, F. Wu, W.-J. Tian and J.-C. Shen, *J. Chem. Soc., Dalton Trans.*, 1999, 4217-4221.
27 W. A. Maza and A. J. Morris, *J. Phys. Chem. C*, 2014, **118**, 8803-8817.
28 Y. Zu and A. J. Bard, *Anal. Chem.*, 2000, **72**, 3223-3232.
29 F. B. Kaufman, A. H. Schroeder, E. M. Engler and V. V. Patel, *Appl. Phys. Lett.*, 1980, **36**, 422-425.
30 K. Shigehara, N. Oyama and F. C. Anson, *J. Am. Chem. Soc.*, 1981, **103**, 2552-2558.
31 H. S. White and A. J. Bard, *J. Am. Chem. Soc.*, 1982, **104**, 6891-6895.
32 S. Lin, Y. Pineda-Galvan, W. A. Maza, C. C. Epley, J. Zhu, M. C. Kessinger, Y. Pushkar and A. J. Morris, *ChemSusChem*, 2016.
33 P.-H. Xie, Y.-J. Hou, B.-W. Zhang, Y. Cao, F. Wu, W.-J. Tian and J.-C. Shen, *Dalton Transactions*, 1999, 4217-4221.

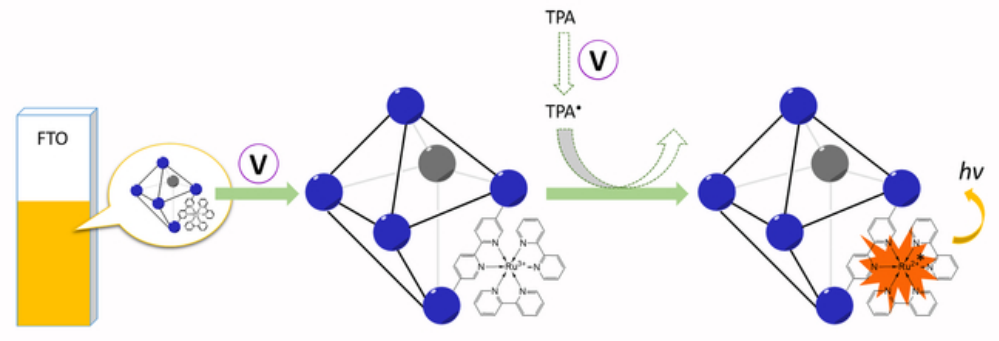

27x9mm (600 x 600 DPI)